Transactions on Computer Science and Intelligent Systems Research
ISSN: 2960-1800, eISSN: 2960-2238 | Volume 7
TPCEE 2024

Optimal line planning for multibeam line measurement based on improved algorithms

Yuanke Meng, Yusheng Lei*, Yikun Kang, Yiyuan Zhao

School of Power and Energy, Northwestern Polytechnical University, Xi'an, China, 710129

* Corresponding Author Email: leiyusheng916@gmail.com

Abstract. In this paper, this paper address the challenges of multibeam line measurement in the sea by first analyzing the correlation between two-dimensional (2D) and three-dimensional (3D) models through the construction of mathematical models. Based on these mathematical models, this paper further develop ocean models and measurement models. These models aid in determining the characteristics of different sea models, as well as the properties of measurement signals under various measurement modes and positions. By employing the models constructed, this paper are able to devise optimal measurement paths and modes for specific bodies of water. Subsequently, this paper identify the best measurement methods and their corresponding limitations within those particular waters. Analyzing the optimal measurement techniques and their associated deficiencies in specific waters allows us to draw final conclusions about the measurements taken in those waters. The multibeam line model finds significant applications in numerous fields, encompassing marine topographic mapping, marine ecological research, marine resource exploration, marine environmental monitoring, and marine engineering and harbor construction. In these application areas, multibeam line measurements provide precise and detailed data support, offering critical tools for the effective understanding and management of our marine environments.

Keywords: Cartesian Coordinate System; Least Squares Method; LU Decomposition Method; Fitting Surface Method; Rotation Matrix; Path Function.

1. Introduction

Since the 1970s, multibeam technology has significantly improved the efficiency and accuracy of marine mapping[1], finding wide applications in sectors like China's military and offshore oil and gas[2]. Yangtze River channel surveys have validated the high resolution and precision of this technology, innovative techniques have enhanced the thoroughness of the surveys, customized systems meet the unique demands of polar and shallow-water areas, sound speed correction and cross-checking ensure data integrity, and the multi-beam system is superior to single-beam systems due to its extensive coverage and high measurement accuracy.

In the 1970s, foreign countries began to study and popularize this system. In recent years, the domestic multibeam measurement technology has developed rapidly. Wang Xiaolong et al[3] studied the method of multibeam tilt installation and proposed to increase the number of beams to realize full coverage measurement underwater. Wang Maomei[4] and other researchers calculated the main technical parameters required to realize full-coverage underwater terrain measurement by analyzing the multibeam measurement data. Wang Fengfan et al[5] designed a polar-oceanic multibeam measurement line laying system to effectively improve the design efficiency of multibeam measurement program. Wang Q et al[6] explored the difficult point in data processing - the sound velocity correction method of shallow water multibeam bathymetry data, and solved the problem of shallow water multibeam bathymetry data processing. Sun Xinxuan et al[7] proposed a multibeam bathymetry data quality assessment method based on cross-checking, which solved the current problem of multibeam bathymetry data quality assessment.

Single-beam depth measurement calculates water depth by measuring the round-trip time of sound waves, while the multi-beam system emits multiple beams to cover a wider area, thereby improving the accuracy and completeness of seabed mapping.

2. The main principle of multibeam measurement

The multi-beam survey system displays underwater terrain by vertically emitting fan-shaped beams and receiving echoes from the seabed. The processed data is used to calculate water depth and create maps, with a wide scanning range and adjustable opening angle that accommodate various terrains and enhance efficiency.

Based on the information in the previous assumptions. The established sea model is shown in Figure 1.

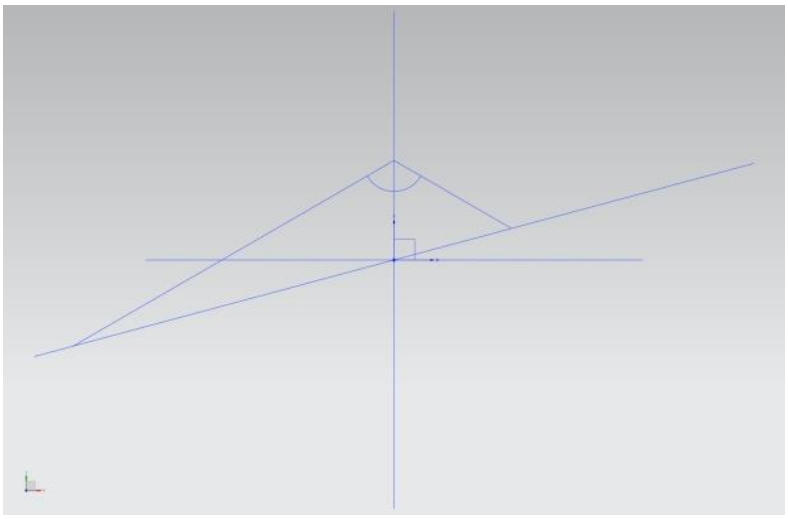

Fig. 1 Two-dimensional map of sea coordinates

Measurement of the ship's position is $A(200i, y_0)$ $(i=-4,-3\mathrm{L}\ 3,4; y_0=70)$. In by the opening angle of the multibeam transducer is $\theta=120^o$, the vector is obtained $\overrightarrow{AT}=(-\sqrt{3},-1)$ $\overrightarrow{AR}=(\sqrt{3},-1)$ and the corresponding linear equation is:

$$l_{AT}:\frac{x-200i}{-\sqrt{3}}=\frac{y-y_0}{-1} \tag{1}$$

$$l_{AT}:y=\frac{x-200i}{\sqrt{3}}+y_0 \tag{2}$$

$$l_{AR}:\frac{x-200i}{\sqrt{3}}=\frac{y-y_0}{-1} \tag{3}$$

$$l_{AR}:y=-\frac{x-200i}{\sqrt{3}}+y_0 \tag{4}$$

Also the equation for sea level is:

$$y=tan\,\alpha\,x \tag{5}$$

The joint equations (2) (4) (5)

The coordinates of T and R are obtained:

$$\left(\frac{\sqrt{3}y_0-200i}{\sqrt{3}\tan\alpha-1},\frac{\tan\alpha\left(\sqrt{3}y_0-200i\right)}{\sqrt{3}\tan\alpha-1}\right) \tag{6}$$

$$\left(\frac{\sqrt{3}y_0+200i}{\sqrt{3}\tan\alpha+1},\frac{\tan\alpha\left(\sqrt{3}y_0+200i\right)}{\sqrt{3}\tan\alpha+1}\right) \tag{7}$$

The depth of seawater at each position is obtained from equation (5), with x obtaining different values at different positions.The coverage width, i.e., the distance between T and R, has:

$$\left|\overrightarrow{AR}\right| = \frac{1}{\cos\alpha}\left|\frac{\sqrt{3}y_0 + 200i}{\sqrt{3}\tan\alpha + 1} - \frac{\sqrt{3}y_0 - 200i}{\sqrt{3}\tan\alpha - 1}\right| \tag{8}$$

Find the coverage width at each of the different locations due to the differences.

Overlap rate between two neighboring signals $\eta = 1 - \frac{d}{W}$ (included among these $d = 200m$ is pace, W is the measured coverage area of A_{I+1}).

The final results are obtained as shown in Table 1.

The overlap rate between two neighboring signals $\eta = 1 - \frac{d}{W}$ (where $d = 200m$ is the step size and W is the A_{I+1} measurement coverage area). The final result is obtained as shown in Table 1.

Table 1. Table of final solution results

Distance of the line from the center/m	-800	-600	-400	-200
Sea depth/m	49.051263	54.288447	59.525631	64.762816
Coverage width/m	315.813328	297.627561	279.441793	261.256025
Overlap with previous line/%	——	0.328019	0.284287	0.234467

0	200	400	600	800
70	75.237184	80.474369	85.711553	90.948737
243.070257	224.88449	206.698722	188.512954	170.327187
0.177193	0.110655	0.032408	-0.060935	-0.174211

3. Multibeam feature solving in three dimensions with different slopes

In the 3D marine area model, by establishing a spatial rectangular coordinate system and combining the ship's heading, multi-beam transducer opening angle, and seabed slope, it is possible to calculate the seawater depth and signal coverage range at different positions. The established sea model is shown in Figure 2.

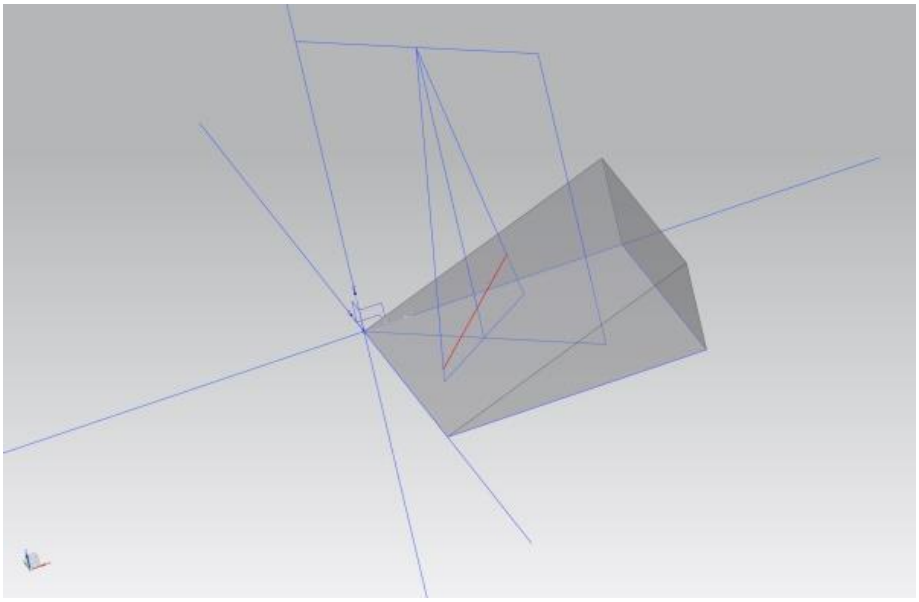

Fig. 2 Three-dimensional sea coordinate map

Forward direction of the boat at point A $\vec{l}=(x_0,y_0,0)$, $\cos\beta=\frac{-y_0}{\sqrt{x_0^2+y_0^2}}$. And because the coordinates of A (x,y,z). Draw a vertical line from A toward the face xoy, $\begin{cases}x=x_1\\y=y_1\end{cases}$, $\vec{l}$ is normal to the scanning surface. Then the equation of the scanning surface is:

$$x_0(x-x_1)+y_0(y-y_1)+z_0(z-z_1)=0 \tag{9}$$

Direction vector of the vertical line over point A $\vec{n_2}=(0,0,-1)$, Let the two boundary direction vectors of the emitted signal $\vec{n}=(m,n,p)$, Then, based on the specific geometric relationships in the topic, the.First $\vec{l}$ with $\vec{n}$ wanting to go vertical, get:

$$x_0m+y_0n=0 \tag{10}$$

This is then obtained from the multibeam transducer with an opening angle of 120◦:

$$\frac{\left|\vec{n}\cdot\vec{n_2}\right|}{\left|\vec{n}\right|\cdot\left|\vec{n_2}\right|}=\cos 60^{o}=\frac{1}{2} \tag{11}$$

Solving Eqs. (2)(4) jointly gives the normal vector as:

$$\vec{n}_{AT}=\left(1,\frac{-x_0}{y_0},\frac{\sqrt{x_0^2+y_0^2}}{\sqrt{3}y_0}\right) \tag{12}$$

$$\vec{n}_{AR}=\left(1,\frac{-x_0}{y_0},\frac{\sqrt{x_0^2+y_0^2}}{-\sqrt{3}y_0}\right) \tag{13}$$

This gives the equation of the line $\vec{AT}$ with $\vec{AR}$:

$$l_{AT}:\frac{x-x_1}{1}=\frac{y-y_1}{\left(\frac{-x_0}{y_0}\right)}=\frac{z-z_0}{\left(\frac{\sqrt{x_0^2+y_0^2}}{\sqrt{3}y_0}\right)} \tag{14}$$

$$l_{AR}:\frac{x-x_1}{1}=\frac{y-y_1}{\left(\frac{-x_0}{y_0}\right)}=\frac{z-z_0}{\left(\frac{\sqrt{x_0^2+y_0^2}}{-\sqrt{3}y_0}\right)} \tag{15}$$

Again, from the coordinate system, the equation of the seafloor slope is:

$$z=y\tan\alpha \tag{16}$$

By solving the coordinates of T and R through simultaneous equations, the problem ultimately boils down to solving a series of linear equation systems. Using the LU decomposition method in a computerized environment can enhance computational efficiency. The model is simplified under special circumstances, that is, when the angle between a straight line and the seabed slope is 0 or 180 degrees, the coverage width can be directly calculated using geometric relations.

The most final signal coverage width (TR) is adjusted for different line direction angles. The final results are obtained as table 2:

Table 2. Table of signal coverage width results

Coverage width/m	Distance/nautical mile from the center of the sea by the survey vessel							
	0	0.3	0.6	0.9	1.2	1.5	1.8	i2.1
Measuring line direction angle/°	0	415.69	466.09	516.49	566.89	617.29	667.69	718.09	768.48
	45	416.19	451.87	487.55	523.23	558.91	594.59	630.27	665.95
	90	416.69	416.69	416.69	416.69	416.69	416.69	416.69	416.69
	135	416.19	380.51	344.83	309.15	273.47	237.79	202.11	166.43
	180	415.69	365.29	314.89	264.50	214.10	163.70	113.30	62.90
	225	416.19	380.51	344.83	309.15	273.47	237.79	202.11	166.43
	270	416.69	416.69	416.69	416.69	416.69	416.69	416.69	416.69
	315	416.19	451.87	487.55	523.23	558.91	594.59	630.27	665.95

4. Optimal solution of the path function for signaling ship navigation

In the further extension of the three-dimensional sea area model, the design of measurement routes to scan the sea area is subject to specific conditions. A three-dimensional right-angle coordinate system is established with the center of the sea area as the origin, the seabed is considered to be a horizontal plane, and the inclination of the horizontal sailing line of the survey vessel is taken into account.The established sea model is shown in Figure 3.

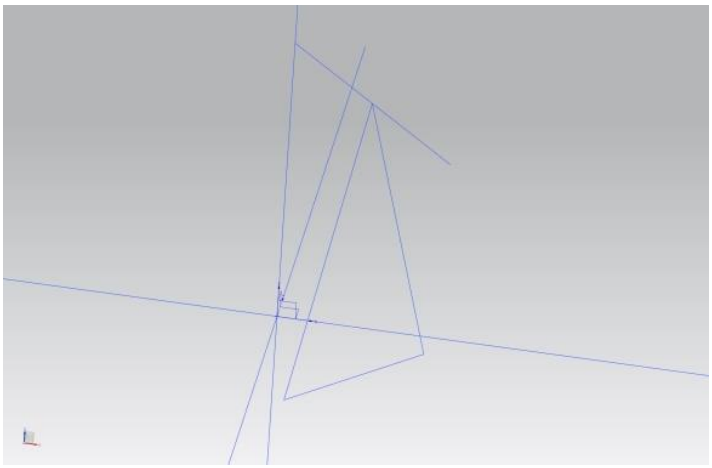

Fig. 3 Diagram of the three-dimensional sea area model constructed in the plane of the seabed

The signaling vessel is measured from $A(0,0,110)$ the point, taking the xoy plane of the seabed, and the horizontal direction vector $\vec{l}=(\sin\beta,-\cos\beta,0)$ of the vessel's travel is set. And the boundary line of the measurement line emitted by A is $\vec{W}_T$ with $\vec{W}_R$. And satisfies $\vec{W}\cdot\vec{l}$ ($\vec{W}$ being the signal emitted, i.e., $\vec{W}_T$ vs. $\vec{W}_R$). The downward unit vector with:

$$\frac{\left|\vec{W}\cdot\vec{n}_0\right|}{\left|\vec{W}\right|\cdot\left|\vec{n}_0\right|}=\cos 60^{o}=\frac{1}{2} \tag{17}$$

From this equation we get $\vec{W}_T$ with $\vec{W}_R$.

Since in the end we need to represent the ship's course correctly in terms of horizontal lines, we need to rotate the present vector to be solved and the point coordinates around the axis by an angle to obtain the transformed vector and point coordinates. In this transformation, we introduce the rotation change matrix:

$$T_{3\times3}=\begin{vmatrix}1 & 0 & 0\\ 0 & \cos\alpha & \sin\alpha\\ 0 & -\sin\alpha & \cos\alpha\end{vmatrix} \tag{18}$$

Then after a change in the coordinate system there is:

$$\begin{vmatrix}x'\\ y'\\ z'\end{vmatrix}=T\cdot\begin{vmatrix}x\\ y\\ z\end{vmatrix} \tag{19}$$

The equation of the seafloor xoy plane in the system: $z=0$. Let the seafloor range be framed by M, N, O, Q, where $M(\lambda_1,0,0)$, $N(\lambda_1,\lambda_2,0)$, $Q(0,\lambda_2,0)$.Additionally construct the vector $\overrightarrow{TA_1M}$.

vectors $\vec{l}$ after a matrix change is($T\cdot\vec{l}$), The vertical vector drawn through M to $T\cdot\vec{l}$ satisfies $\overrightarrow{TL}\cdot\vec{m}=0$,From this we can solve for $\vec{m}$. Also by vector covariance there is a mixed product of three vectors which is 0,i.e. satisfies $\left[\overrightarrow{TA_1}M\,Tl\,m\right]=0$.

At this point, assuming that the survey ship takes a total of N measurements, the path length function measured by the survey ship is:

$$\sum_{i=1}^{N}l_i=\sum_{i=1}^{N}\left(\frac{-1}{\sin\beta}\lambda_1-\frac{W_i(1-\eta)}{\tan\beta}\right) \tag{20}$$

Ultimately, it is sufficient to minimize the total measured path on the basis of this function. However, this function is required by the model to have the following constraints:

Constraint 1:In order to ensure that the starting endpoint of the measurement is within the measurement range, a rotational change to the downward unit vector $\vec{n}_0$ is obtained, so the constraint equation $T\cdot\vec{n}_0$ is:

$$\frac{\left|\vec{m}\cdot\left(T\vec{n}_0\right)\right|}{\left|\vec{m}\right|\cdot\left|\left(T\vec{n}_0\right)\right|}\geq\cos60^{\circ}=\frac{1}{2} \tag{21}$$

For all paths each path is actually scanned with parallel equal lengths l_i, the direction vector is l_0 ,the length of the occlusion-covered portion. $l_0=\frac{(-1)}{\sin\beta}\lambda_1$

Let the overlap rate be η suchthat there are.

$$l_i=l_0-\frac{W_i(1-\eta)}{\tan\beta}=\frac{-1}{\sin\beta}\lambda_1-\frac{W_i(1-\eta)}{\tan\beta} \tag{22}$$

Complete coverage must be satisfied at this point.

Let there be a total of N scans, then also satisfy that the Nth covers the remainder. Then i.e., Q has to satisfy over Q to $\vec{Tl}$ the drape vector $\vec{q}$.There is $\vec{q}\cdot\overrightarrow{TL}=0$ and $\overrightarrow{TA_n}QTl\,\vec{q}=0$.From this we can solve for $\vec{q}$.

Where the coordinates of ship A in the ith scan are given by the following equation:

$$A_i\left(W_i\left(\frac{1}{2}-\eta\right)\cos\beta,\frac{W_i(1-\eta)}{-\sin\beta}i,-110\right) \tag{23}$$

Calculate W_i, i.e.at launch the two boundaries at for $\overrightarrow{TW_T}$ and $\overrightarrow{TW_R}$, and then write the side solution equations by TA_i, $\overrightarrow{TW_T}$ and TA_i $\overrightarrow{TW_R}$, respectively, the two are obtained by solving together with W_i the equation of the submarine plane: TA_i $z=0$ .The trajectory length analysis is plotted in Figure 4.

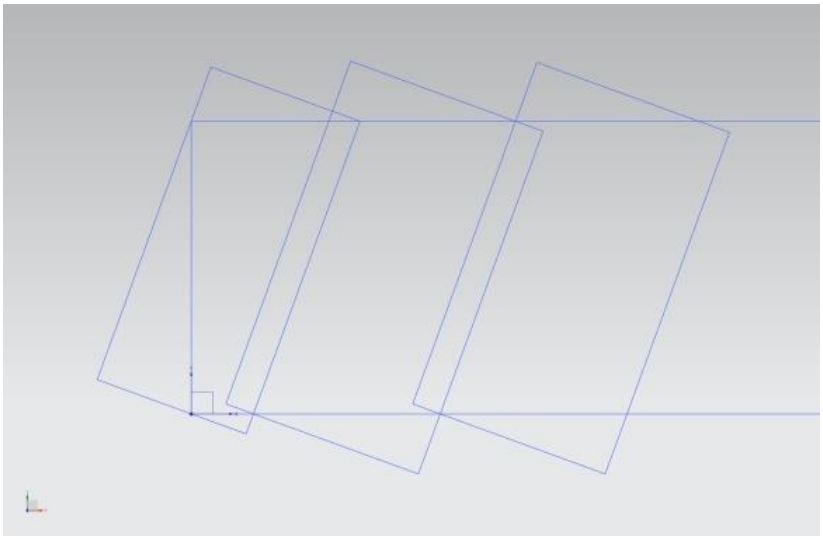

Fig. 4 Plot of trajectory length analysis

Constraint 2:In order to ensure that the termination point is within the scanning range, then there is:

$$1\geq\frac{\left|\vec{q}\cdot\left(\overrightarrow{Tn_0}\right)\right|}{\left|\vec{q}\right|\cdot\left|\left(\overrightarrow{Tn_0}\right)\right|}\geq\cos 60^{\circ}=\frac{1}{2} \tag{24}$$

Constraint 3:Required by the size of the overlap rate in the model, there:

$$0.1\leq\eta\leq 0.2 \tag{25}$$

From this, it is sufficient to find the minimum value of the route length function under these three constraints. Considering the relative complexity of these three constraints, the constraint model is simplified as follows:

A vertical line $l_{始}$ drawn from Q intersects AM at D_1, get a line l_{QD1}, The vertical line $l_{终}$ from M intersects QN at D_2, get a line l_{MD2}, The vertical line W_1 from O intersects MN at D_4, get a line l_{OD4}, Draw a vertical line W_N from N to intersect QD at D_3 and get the line l_{ND3}. The intersection point of the first scan boundary with l_{MD2} is found by W_1 on l_{MD2} and used as a reference to calculate W_2, then the intersection point is found on l_{MD2} to calculate W_3, and so on, until the intersection point sought is not within the area to be measured, i.e. W_N is found, for a total of N times. Since the seafloor is considered to be approximately considered flat under single beam wave measurements, $W_i=2H_i\cdot\tan\frac{\theta}{2}$, H_i are the depths to the seafloor at that point.

This leads to the constraint equation;

$$\left|\overline{MD_2}\right|\leq\sum_{i=1}^{N}W_i(1-\eta_i) \tag{26}$$

$$\left|\overline{QD_2}\right| \le \sum_{i=1}^{N} W_i \left(1-\eta_i\right) \tag{27}$$

The formula for calculating the length of each survey line:

$$l_i = \left|\overline{ND_3}\right| + \frac{\left(\frac{Wi}{2}\right)}{-\tan\beta} \tag{28}$$

where l_i is the length traveled by the ith measurement.

From this, the optimized constraints are derived, and the above calculations are combined to obtain the results of this model.

The final result is that there are 34 survey lines, which are parallel to each other and their directions are basically parallel to the direction of the isobaths, and the length of the shortest survey route is about 122,360 m. The result is that there are 34 survey lines, which are parallel to each other and their directions are basically parallel to the direction of the isobaths.

5. Optimized design of the fitted surface method for typical water areas

5.1. Contextual assumptions and analysis

The typical water model aims to optimize the multibeam scanning path in real waters to achieve the shortest path and meet the signal coverage requirements. Based on the previous model conclusions and reference, the optimal heading of the survey vessel is determined, the optimal multibeam transducer opening angle is selected, and the appropriate angle is screened[8]. The slope is processed by applying the fitted surface method, transformed into a standard slope, solved and the optimal path is determined using the previous model method. The analysis process is shown in Figure 5.

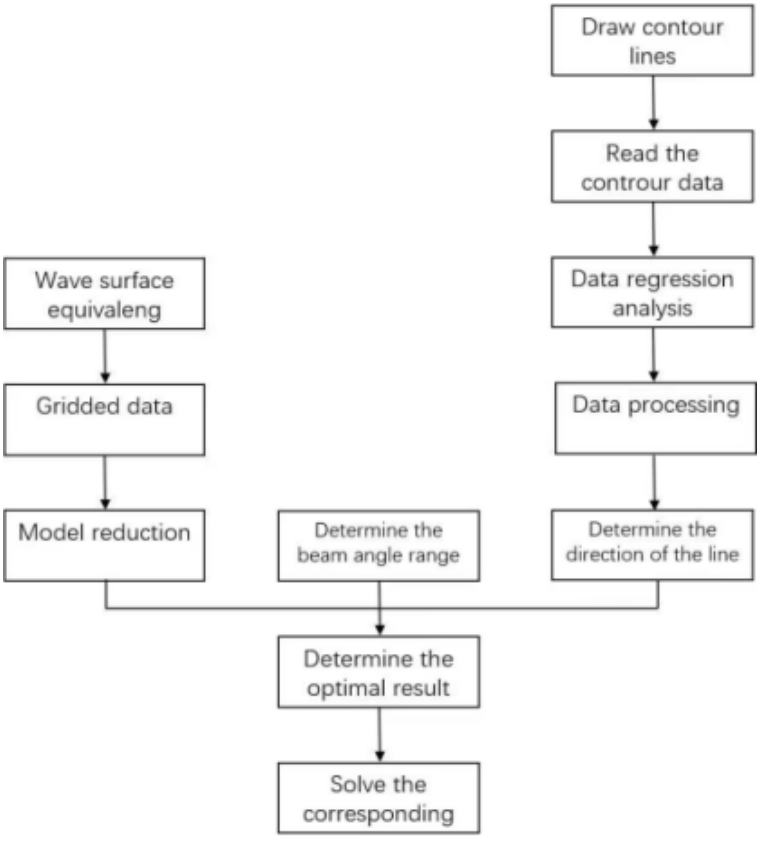

Fig. 5 Typical watershed model analysis flow

The typical water model is a solution to a more realistic seabed model. In this model, optimal survey lines need to be laid out to scan the seafloor and, at the same time, find the optimal solution for the three objective functions that need to be solved. A typical water model can be given as an example to solve, and the isobaths of the seafloor model are shown in Figure 6:

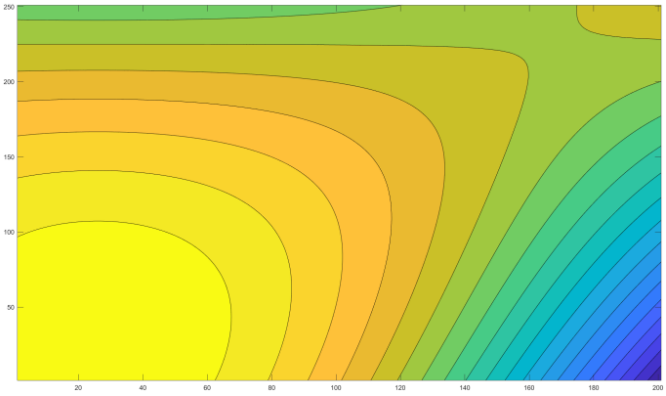

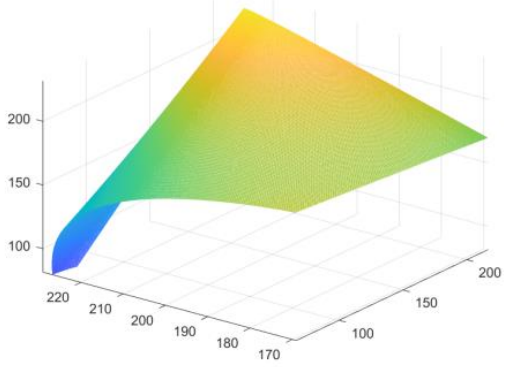

Fig. 6 Seafloor isobaths **Fig. 7** General topographic map of the seabed

In the typical water model, from the sailing path model and the conclusions of reference[9], in order to maximize the coverage of the sea area and shorten the length of the survey line, the sailing direction of the multibeam survey vessel should be the same as the direction of the isobath extension. The slope of the survey line direction was determined by least squares fitting of the contour map. The fitting process is described below:

First, the general extension direction of the isobath is found. The general topography of the seafloor is shown in Figure 7.

The horizontal and vertical coordinate data of a number of points on each isobath were read through MATLAB, and the data obtained from each isobath were fitted by linear regression using the least-squares method, respectively, and the final fitting results are shown in the table 3:

Table 3. Results of isobathymetric regression fitting

serial number	regression equation
1	y = -1.1863x + 130.71
2	y = -1.3135x + 182.89
3	y = -0.9104x + 205.04
4	y = -0.4059x + 216.7
5	y = -0.1768x + 226.99
6	y = 2.1766x - 203.6
7	y = 0.068x + 231.98
8	y = 2.2981x - 265.35
9	y = 2.4156x - 286.81
10	y = 2.4711x - 325.48
11	y = 2.514x - 356.92
12	y = 2.5488x - 383.86
13	y = 1.9501x - 286.48
14	y = 2.0498x - 322.33
15	y = 2.1338x - 354.03
16	y = 2.201x - 381.53
17	y = 2.258x - 406.3
18	y = 2.3035x - 428.19
19	y = 2.3848x - 468.44
20	y = 2.354x - 450.5

This resulted in a set of slope data, of which outliers were then eliminated from the process. This is shown in Table 4:

Table 4. Outlier rejection results

Outlier number	regression equation
4	y = -0.4059x + 216.7
5	y = -0.1768x + 226.99
7	y = 0.068x + 231.98

The direction of the survey line is shown in Figure 8, and the seafloor topography was analyzed by isobath map and divided into sparse contour zones with gentle slopes and dense contour zones with steep slopes. Due to the complexity of the terrain, quadratic surface fitting is not applicable, so the equivalent terrain method is used. The sea area is divided into two parts, each of which is equivalent, and then the navigation path model is applied to solve the problem.

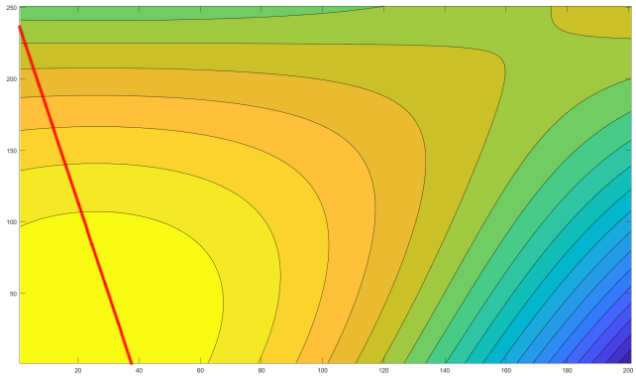

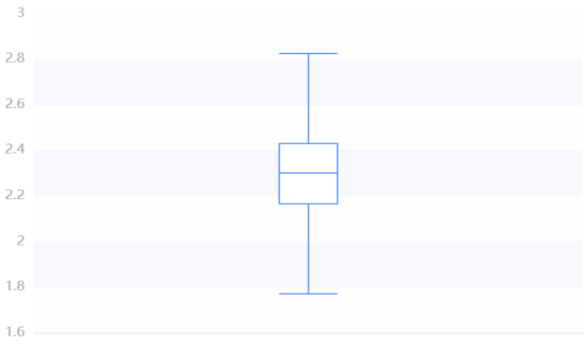

Fig. 8 Measurement direction diagram **Fig. 9** Right part of the data box diagram

After simplifying the seabed into two slopes, the formula for the slope is obtained from reference as $Slope = \sqrt{Slope_x^2 + Slope_y^2}$ (where $Slope$ is the slope, $Slope_x$ is the slope in the x-direction and $Slope_y$ is the slope in the y-direction) In turn, the curved seafloor can be fitted to two planes[9].

In the typical marine model, data analysis determined the average sea depth and boundary line position, and calculated the regression equation slope. Descriptive statistical analysis and box plots were used to assess data stability and outliers. A box plot of the data on the right-hand side is shown in Figure 9. Optimal survey paths were determined based on three objective functions to minimize total length, areas with overlap exceeding 20%, and the ratio of missed survey area to total area. Routes were established using a specific method, and total length, coverage overlap rate, and missed survey area were calculated. The equation of the survey line can be expressed in the coordinate system as $y = kx + \frac{d_i}{\tan\theta}$ where d_i denotes the distance between the i line and the $i+1$ line of measurement, and the normal perpendicular to it can be expressed as $y = -\frac{1}{k} + 5 - \frac{j \cdot \left(5 - \frac{4}{k}\right)}{M}$ which j is an integer from 1 to M, The larger M is, the more normals are taken, the higher the precision is, but at the same time the complexity of the operation is also higher. Based on the requirements of precision and computational complexity, the value of M here takes the order of magnitude of 10^4. The measured line is then associated with the normal to solve for the coordinates of all intersections, and the closest known point to the intersection is found as the approximate location of the intersection by rounding down the value of the intersection coordinates. This is followed by the formula $W_i = 2H_i \cdot \tan\frac{\theta}{2}$ Get the scan width at

this point W_i, Then from the defining equation of the overlap rate $\eta = 1 - \frac{d}{W}$,it is possible to find the overlap rate for each point. Here if $\eta > 20\%$ means that the overlap rate exceeds the expected requirement. if $\eta \le 0$, it means that there is a missed measurement. After calculations, there are n_1 points corresponding to the fulfill $\eta > 20\%$, while there are n_2 points corresponding to the fulfill $\eta \le 0$. Thus the three objective functions are expressed as:

$$\min\left[\sum_{i=1}^{N} l_i\right] \tag{29}$$

$$\min\left[n_1 \cdot \frac{5-\frac{4}{k}}{M} \cdot \sin\left(\tan^{-1} k\right)\right] \tag{30}$$

$$\min\left[\frac{\frac{5-\frac{4}{k}}{M} \cdot \sin\left(\tan^{-1} k\right) \cdot \sum_{j=1}^{n_2}\left(\left|\eta_j\right| \cdot w_i\right)}{4 \times 5}\right] \tag{31}$$

Through the calculation and comparison of these three objective functions, and the beam opening angle θ in a certain range of some representative values can be calculated to obtain the optimal value of the three conditions taken into account, that is, the optimal solution of this problem.

According to reference, it is known that with the survey vessel sailing at a normal speed[10]. When the beam angle θ is greater than 140^o, the quality and accuracy of the measurement data is low.Therefore, it is necessary to limit the opening angle θ to and below 140^o for simulation and the specific results obtained are shown in table 5:

Table 5. Lengths of survey lines at some different beam angles

Field angle/degree	Line length/meter
140	347328
120	572480
110	703730
100	853730
90	1022310
80	1228730
70	1472430
60	1809910

It can be seen that the larger the beam angle, the shorter the length of the line, so 140^o is the optimal beam angle. At this time, the total length of the measurement line is 347328m, and the length of the missed measurement area accounting for 2.9% and the overlap rate is more than 20% is 237155.6m.

6. Conclusion

This study explores the application of multibeam technology in marine mapping and analysis, focusing on its efficiency and accuracy enhancements over traditional single-beam systems. It begins with an introduction to multibeam technology, highlighting its evolution since the 1970s and its widespread applications in sectors such as military operations and offshore resource exploration. The main principle of multibeam measurement is discussed, detailing how the technology uses fan-shaped beams to gather data on underwater terrain, calculate water depth, and create detailed maps. The study

emphasizes the flexibility of multibeam systems in accommodating various terrains and enhancing operational efficiency.The research extends into 3D modeling, where it integrates ship orientation, transducer angles, and seabed slopes to calculate water depth and signal coverage across different positions. Techniques like LU decomposition are employed to streamline computational processes and improve model accuracy.Further, the study addresses optimal survey route design using path functions, considering constraints like coverage area and overlap rates. It explores methods to minimize survey path length while ensuring complete coverage of the marine area under study.Lastly, the study introduces the fitted surface method tailored for typical water areas, optimizing survey paths based on the direction of isobaths and seabed slopes. It employs least squares fitting to determine the optimal path of survey vessels and beam angles, ensuring efficient data collection and minimizing survey length.

References

[1] Yan guanfa, Wan luhe, Wen zhihong. Slope aspect analysis of vegetation distribution in Tianchi in Changbai Mountain based on RS and DEM[C]. Selected Papers of the 4th "Frontier Technology Forum of Surveying and Mapping Science". Bulletin of Surveying and Mapping,2012:240-243+246. (in Chinese)

[2] LI Sen, QU Jizhou, LI Dong. Effects of multibeam sector opening angle and ship speed on the quality of collected data[J]. Chinese Science and Technology Journal Database (full text version) Engineering Technology,2020(12):0246-0247. (in Chinese)

[3] WANG Xiao-long, LI Tao. Application of multi-beam tilt installation technology in underwater detection engineering[J]. Port & Waterway Engineering, 2020, (S1):30-34. (in Chinese)

[4] WANG Maomei, ZHOU Guangyu, CHEN Nan, et al. Multi-beam measurement technology based on high resolution[J] . Water Resources and Hydropower Engineering, 2021, 52(S2) : 385-389.

[5] Wang Fengfan, Ma Yong. Design and Implementation of a Multi-beam Sonar Survey Line Layout System for Polar Oceans[J]. Marine Information Technology and Application, 2023, 38(03): 158-162+186.

[6] WANG Qi, LIU Shengxuan, GUAN Yongxian. The discussion on shallow multibeam echosounding data processing method [J]. Hydrographic Surveying and Charting,2021,41(2):29-33.

[7] SUN Xinxuan, TONG Jie, LI lei. Research on the uncertainty of multi-beam water depth[J]. Journal of Geomatics,2019,44(6):49-50.

[8] GB 12327-2022, Specifications for Hydrographic Surveying[S].

[9] Bathymetric survey[J] . Ocean Information Technology and Applications, 2023, 38(3): 158-162+186.

[10] Shu Shengyuan, Cheng Long. Application analysis of multi-beam system in Yangtze River waterway survey[J]. China Water Transport,2017,38(9):46-47.)